

**Characterization and atomic modeling of an asymmetric grain boundary**Hak-Sung Lee,<sup>1</sup> Teruyasu Mizoguchi,<sup>2,\*</sup> Takahisa Yamamoto,<sup>3,4</sup> Suk-Joong L. Kang,<sup>5</sup> and Yuichi Ikuhara<sup>1,4,†</sup><sup>1</sup>*Institute of Engineering Innovation, The University of Tokyo, 2-11-16, Yayoi, Bunkyo, Tokyo 113-8656, Japan*<sup>2</sup>*Institute of Industrial Science, The University of Tokyo, 4-6-1, Komaba, Meguro, Tokyo 153-8505, Japan*<sup>3</sup>*Department of Advanced Materials Science, The University of Tokyo, 5-1-5, Kashiwanoha, Kashiwa, Chiba 277-8561, Japan*<sup>4</sup>*Nanostructures Research Laboratory, Japan Fine Ceramics Center, 2-4-1, Mutsuno, Atsuta-ku, Nagoya 456-8587, Japan*<sup>5</sup>*Department of Materials Science and Engineering, Korea Advanced Institute of Science and Technology, 373-1, Gusongdong, Yusong-ku, Daejeon, Republic of Korea*

(Received 24 October 2011; published 23 November 2011)

Grain boundaries (GBs) significantly affect the properties of materials. In an effort to examine the phenomena at GBs, many model boundaries, typically symmetric tilt GBs, have been investigated. However, the geometries of symmetric tilt GBs are too restricted to represent commonly occurring interface phenomena properly in polycrystalline materials. Thus, a method of applying density functional theory (DFT) to asymmetric GBs has long been desired. Here, we present a simple geometric method and a new GB model with two surfaces which make it possible to characterize an asymmetric tilt GB and calculate the GB energetics. Our method can be extended to study other geometric asymmetric interfaces in various materials. The proposed technique thus paves the way for DFT-related studies of asymmetric interfaces.

DOI: [10.1103/PhysRevB.84.195319](https://doi.org/10.1103/PhysRevB.84.195319)

PACS number(s): 61.72.Mm, 68.35.Ct

**I. INTRODUCTION**

The characterization of grain boundaries (GBs) at the atomic level is a fundamental subject in materials science and solid-state physics because the GB drastically affects the physical properties of polycrystalline materials. The effects of GBs on the material properties become more significant in nanocrystalline materials designed for catalysts, fuel cells, lithium ion batteries, and other such devices. Thus, GBs, in particular symmetric tilt GBs, have been extensively investigated experimentally as well as theoretically with respect to their atom arrangement, termination plane, chemical composition, and electronic structure.<sup>1–14</sup> In contrast, studies of asymmetric tilt GBs have only occasionally been done, despite the fact that they are more frequently observed than symmetric tilt GBs<sup>15</sup> and more significantly affect the material properties.<sup>16</sup> Experimental observations of asymmetric tilt GBs of some ceramics<sup>16–22</sup> and metals<sup>23–25</sup> have been attempted; however, the atomic arrangement of GB cores has not been clarified. Structure calculations of asymmetric tilt GBs for metals<sup>3,26,27</sup> have been done, but those for complex ceramics such as SrTiO<sub>3</sub> along with the energies of their asymmetric boundaries have yet to be formulated. The present study reports the atomic modeling and structure calculation of an asymmetric GB as well as its experimental confirmation in SrTiO<sub>3</sub>. This result is the first experimental and theoretical determination of the atomic arrangement and energetics of asymmetric GB cores in complex ceramics.

To calculate the structure of an asymmetric GB, we first constructed an atomic model and periodic lattice structures with [001](100)//(430) SrTiO<sub>3</sub> asymmetric tilt GBs, taking advantage of a special geometry based on Pythagorean numbers. This model asymmetric tilt GB allows us to construct a calculation cell whose size is suitable for density functional theory (DFT) calculations. The advantage of this structure also lies in the modeling of a calculation structure without misfit, unlike in a previous investigation.<sup>20</sup> We formulated first-principles calculations for the constructed asymmetric

boundary models to identify the energetically most stable boundary structure and fabricated the asymmetric tilt boundary using two single crystals with (100) and (430) planes, characterizing its atomic structure by high-angle annular dark-field scanning transmission electron microscopy (HAADF-STEM). By combining first-principles calculations and atomic resolution observations, we were able to identify the atomic structure and evaluate the GB energy of the [001](100)//(430) asymmetric tilt GB in SrTiO<sub>3</sub>.

**II. METHODOLOGY**

The first-principles projector augmented wave (PAW) method, within a generalized gradient approximation (GGA) implemented in the VASP code,<sup>28,29</sup> was used for the calculation. Wave functions were expressed in the plane-wave basis set with a cutoff energy of 330 eV. The optimized lattice constant of perfect crystalline SrTiO<sub>3</sub> was calculated with a 10 × 10 × 10 k-point mesh generated by the Monkhorst-Pack scheme (35 irreducible k points) and was found to be 3.942 Å. To calculate GB structures, a 1 × 1 × 3 k-point mesh generated by the Monkhorst-Pack scheme was used and the GB structure was relaxed until the residual force was less than 0.1 eV/Å.

A undoped SrTiO<sub>3</sub> bicrystal fabricated by rotating two single crystals (Furuichi Co., Ltd.) at orientations of 0° and 36.8° about the [001] direction was used in this study. The size of the bicrystal was 10 × 10 × 0.5 mm. TEM samples were fabricated by the conventional method, including mechanical polishing, dimple grinding, and ion-beam thinning. The GB structure at the atomic level was observed by STEM [JEOL JEM-2100F with a spherical aberration corrector (CEOS GmbH)] with a probe-forming aperture of 23 mrad and with a HAADF detection range of 81 to 221 mrad. In the HAADF-STEM system, a focused electron beam was scanned across the specimen and the highly diffracted electrons were collected by an annular detector.

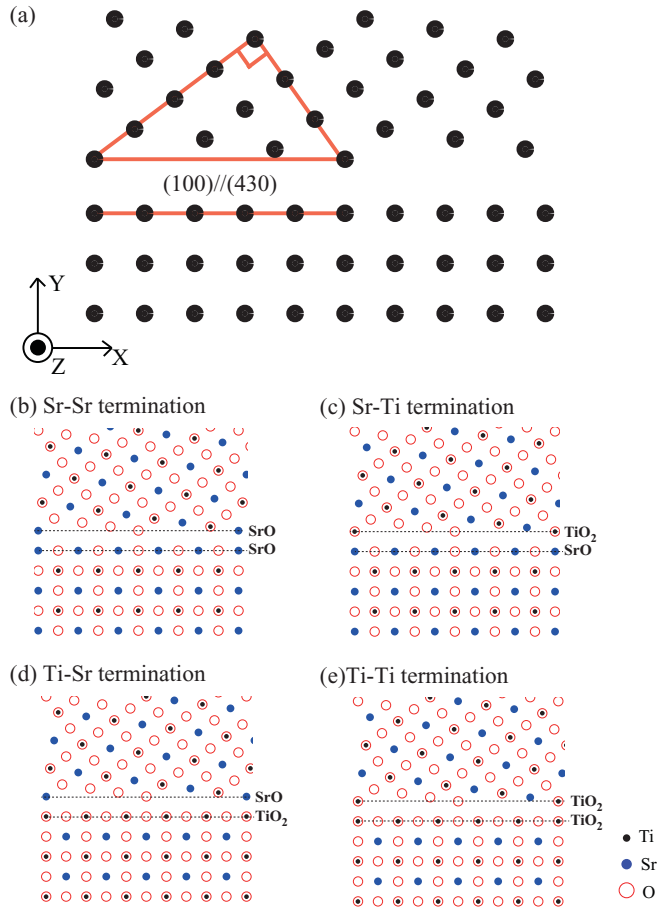


FIG. 1. (Color online) A lattice model and atomic structures of [001](100)//(430) GB in SrTiO<sub>3</sub>. (a) Lattice geometry of asymmetric tilt [001](100)//(430) GB. With the help of simple geometry (Pythagoras' theorem), a periodic structure can be fabricated without misfit. (b)–(e) Boundary structures of different terminations: (b) Sr-Sr, (c) Sr-Ti, (d) Ti-Sr, and (e) Ti-Ti. The former element represents the termination of the (100) plane and the latter element represents the termination of the (430) plane.

### III. RESULTS AND DISCUSSION

#### A. Modeling of the asymmetric tilt GB: [001](100)//(430) SrTiO<sub>3</sub> GB

The atomic structure of the [001](100)//(430) asymmetric tilt GB in SrTiO<sub>3</sub> was calculated by the first-principles projector augmented wave (PAW) method implemented in the VASP code.<sup>28,29</sup> The lattice model was constructed as shown in Fig. 1(a). Here, the  $x$  and  $y$  directions were set parallel and perpendicular to the GB plane, respectively, with the tilting axis defined along the  $z$  direction. As the plane indices satisfy the Pythagoras condition—the periodicity of the atomic arrangement in the (430) plane is exactly equal to five times the periodicity in the (100) plane—a periodic structure with no misfit is produced. As the (100) and (430) planes are not stoichiometric surfaces, four initial structures with different terminations, Sr-Sr, Sr-Ti, Ti-Sr, and Ti-Ti, were considered, as shown in Figs. 1(b)–1(e). For instance, the GB unit cell with the Sr-Sr termination [Fig. 1(b)] consists of 36 Sr, 30 Ti, and 156 O atoms. Thus, it can be said to be in a 6 SrO excess state

or 6 TiO<sub>2</sub> deficient state. Similarly, the other GBs shown in Figs. 1(c)–1(e) are also not stoichiometric.

As a reference state for translation at each termination, the structure for which the cation locations in the (430) plane termination match those in the (100) plane termination was selected, as shown in Figs. 1(b)–1(e). Figure 2(a) depicts the calculation cell of the Ti-Ti termination structure without translation. Each calculation system consists of two grains, Grain A and Grain B, along with two GBs, GB1 and GB2. The model structures for the other terminations were constructed in a similar manner. As the two GBs, GB1 and GB2, are identical for structures with no translation, the GB energy can be calculated by the following equation:

$$\begin{aligned} \gamma_{\text{GB}}(0) &= \frac{E_{\text{Total\_2GB}} - n_{\text{Sr}}\mu_{\text{Sr}} - n_{\text{Ti}}\mu_{\text{Ti}} - n_{\text{O}}\mu_{\text{O}}}{2A} \\ &= \frac{E_{\text{Total\_2GB}} - n_{\text{SrTiO}_3}\mu_{\text{SrTiO}_3} - n_{\text{SrO}}\mu_{\text{SrO}}}{2A} \\ &= \frac{E_{\text{Total\_2GB}} - n'_{\text{SrTiO}_3}\mu_{\text{SrTiO}_3} - n_{\text{TiO}_2}\mu_{\text{TiO}_2}}{2A}, \end{aligned} \quad (1)$$

$(n'_{\text{SrTiO}_3} = n_{\text{SrTiO}_3} + n_{\text{SrO}}).$

Here,  $E_{\text{Total\_2GB}}$  denotes the total energy of the two identical GBs without translation, and  $n_{\text{Sr}}$ ,  $n_{\text{Ti}}$ , and  $n_{\text{O}}$  are, respectively, the numbers of Sr, Ti, and O atoms at the boundary.  $A$  denotes the area of the GB, and  $n_{\text{SrO}}$  and  $n_{\text{TiO}_2}$  represent the excess or deficient numbers of SrO and TiO<sub>2</sub>, respectively, with respect to the stoichiometric composition. The GB energy with nonstoichiometric compositions could be estimated by considering the excess chemicals.<sup>9</sup> The calculated boundary energies are presented in terms of the chemical potential of SrO in Fig. 3(e). The chemical potential of one Ti and two O atoms in SrTiO<sub>3</sub> is the difference in the chemical potential between SrTiO<sub>3</sub> and the Sr and O atoms,  $\mu_{\text{TiO}_2} = \mu_{\text{SrTiO}_3}^{\text{Bulk}} - \mu_{\text{SrO}}$  (in SrTiO<sub>3</sub>). In order to estimate the chemical potentials of the Sr, Ti, and O atoms in SrTiO<sub>3</sub>, the free energies of Sr (metal), Ti (metal), SrO (solid), TiO<sub>2</sub> (solid), O<sub>2</sub> (gas), and SrTiO<sub>3</sub> (bulk) were calculated. The details of these calculations were described in our previous reports.<sup>4,5</sup>

The chemical potential of TiO<sub>2</sub> in the calculation cell can be estimated in an oxidizing condition. It varies within the following range:<sup>9</sup>

$$\mu_{\text{SrTiO}_3}^{\text{Bulk}} - \mu_{\text{SrO}}^{\text{Bulk}} \leq \mu_{\text{TiO}_2} \leq \mu_{\text{TiO}_2}^{\text{Bulk}} = g_{\text{TiO}_2}^0. \quad (2)$$

When an arbitrary translation along the  $x$  direction is applied, GB1 and GB2 in the calculation cell are no longer identical. To estimate the GB energies with these types of translated configurations and to find the most stable structure, a new model containing only one GB and two surfaces was considered [Figs. 2(b) and 2(c)]. By considering the total-energy difference between the states with and without translation, the relative GB energy between the two states was calculated. In this case, the GB energy of the translated structure can be estimated by the equation

$$\gamma_{\text{GB}}(x) = \gamma_{\text{GB}}(0) + \frac{E_{\text{Total\_Surface}}(x) - E_{\text{Total\_Surface}}(0)}{A}, \quad (3)$$

where  $E_{\text{Total\_Surface}}(x)$  is the total energy of the structure shown in Fig. 2(c) with  $x$  translation.  $\gamma_{\text{GB}}(0)$  is the GB energy estimated by Eq. (1) for each termination. Because this model

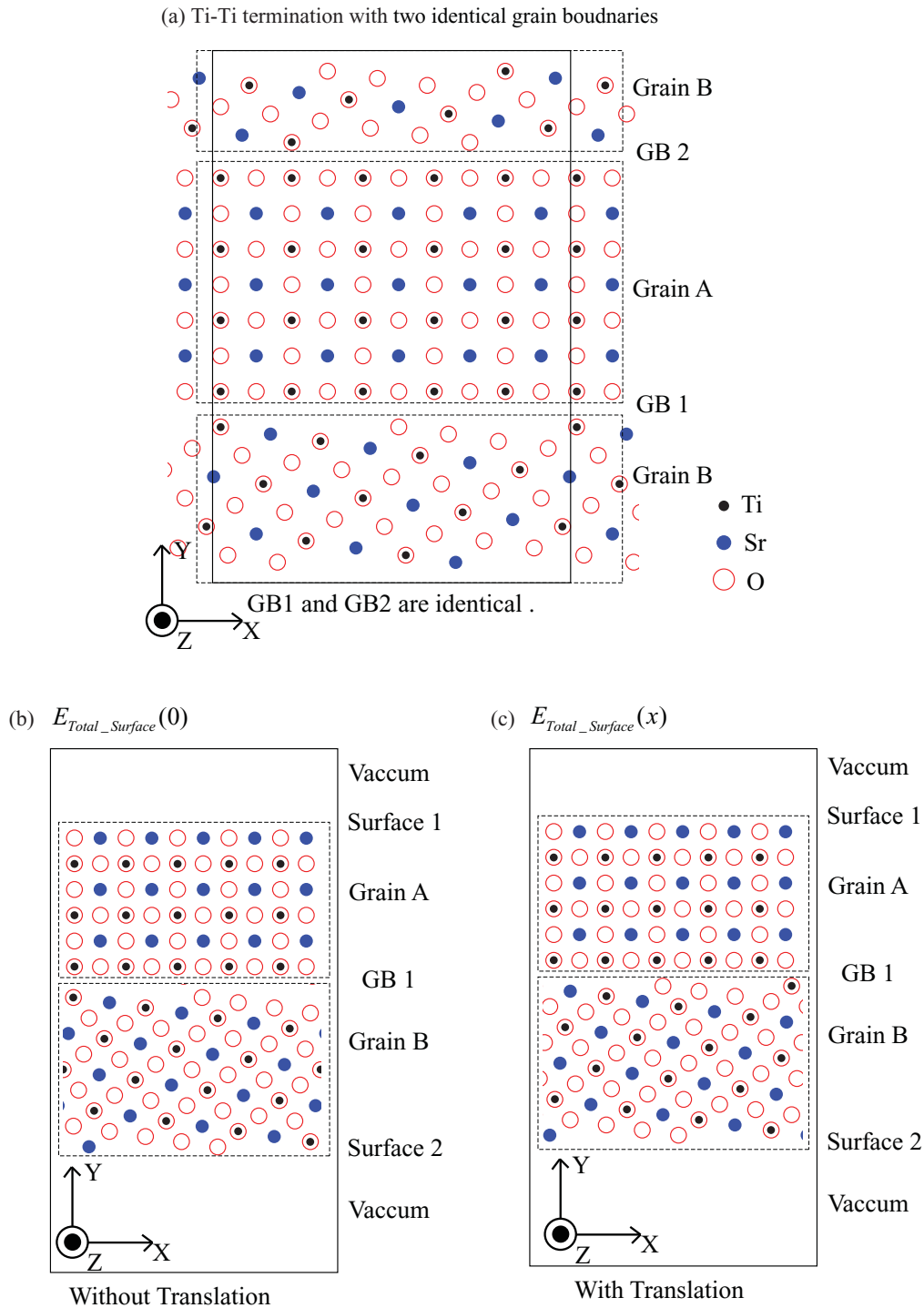


FIG. 2. (Color online) Model structures for calculating GB energies with rigid-body translations: (a) Ti-Ti terminated [001](100)//(430) GB model with two identical GBs without translation. (b) and (c) GB model structures with one GB and two surfaces with (b) no translation and (c) with a translation of 1.5 Å in the  $x$  direction.

includes two surfaces, it is necessary to estimate the effect of the surfaces on the GB energy. The validity of the present method was checked by calculating the GB energy with a structure translated along the  $z$  direction. Given that translation along the  $z$  direction does not break the symmetry of the two grain boundaries, GB1 and GB2, the surfaces were not necessary to estimate the GB energy. The maximum difference

between the GB energies in the two different methods, with and without surfaces, specifically the error introduced by the presence of two surfaces, was less than 0.05 J/m<sup>2</sup>, indicating that the present method feasibly estimates the GB energy.

Figures 3(a)–3(d) show the calculated GB energies for the Sr-Sr, Sr-Ti, Ti-Sr, and Ti-Ti terminations. The GB

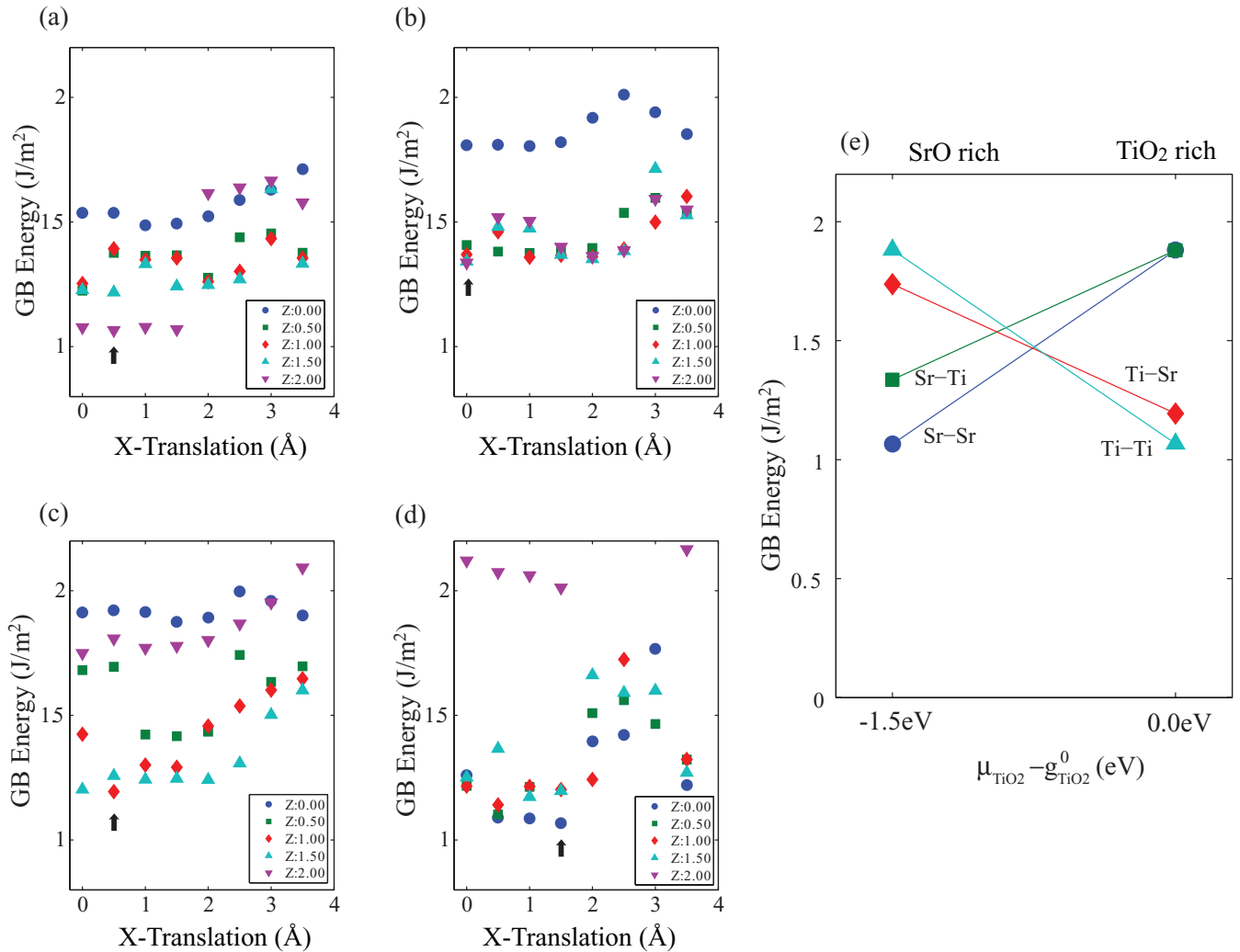


FIG. 3. (Color online) Calculated GB energies as a function of the rigid-body translation. (a) and (b) Variations of GB energies with (a) Sr-Sr and (b) Sr-Ti terminations with rigid-body translation under the SrO-rich condition. The lowest GB energy is indicated by an arrow. (c) and (d) Variations of GB energies with (c) Ti-Sr and (d) Ti-Ti terminations with translation under the TiO<sub>2</sub>-rich condition. The lowest GB energy is indicated by an arrow. (e) The lowest GB energies among all rigid-body translation configurations for different terminations. The Ti-Ti termination exhibits the lowest GB energy in the Ti-rich condition and the Sr-Sr termination does so in the Sr-rich condition.

energies vary significantly depending on the translation, and the structures without translation do not always give the lowest GB energy. This result indicates that translation between the two grains is essential to determine the stable boundary structure of the asymmetric GBs.

The most stable translation states for the GBs with the Sr-Sr, Ti-Sr, Sr-Ti, and Ti-Ti terminations were  $(x, y, z) = (0.5, 2.0, 2.0 \text{ \AA}), (0.0, 2.0, 2.0 \text{ \AA}), (0.5, 2.0, 1.0 \text{ \AA}),$  and  $(1.5, 0.0, 0.0 \text{ \AA}),$  respectively. For the most stable GB structures, the variation of the GB energy with the chemical potential of SrO was calculated, as shown in Fig. 3(e). Because the number of excess or deficient SrO compounds is different for different terminations, each termination shows a different variation in the plots in Fig. 3(e). The GB energy of the Sr-Sr termination varies from 1.06 J/m<sup>2</sup> under the SrO-rich condition to 1.87 J/m<sup>2</sup> under the TiO<sub>2</sub>-rich condition. In contrast, the GB energies of the Ti-Sr and Ti-Ti terminations are, respectively, 1.26 and 1.08 J/m<sup>2</sup> under the TiO<sub>2</sub>-rich

condition, which are lower than those under the SrO-rich condition of 1.81 and 1.89 J/m<sup>2</sup>. Note that the GB energies of the most stable asymmetric [001](100)/(430) GB under the TiO<sub>2</sub>-rich oxidizing condition are quite similar to that (0.98 J/m<sup>2</sup>) of the symmetric tilt [001](210)  $\Sigma 5$  GB, as well as to that (0.93 J/m<sup>2</sup>) of the [001](310)  $\Sigma 5$  GB under the same calculation condition.<sup>4,5</sup> For [001](210)  $\Sigma 5$ , three possible terminations, SrO-SrO, SrO-TiO<sub>2</sub>, and TiO<sub>2</sub>-TiO<sub>2</sub>, were considered, while for [001](310)  $\Sigma 5$ , the stoichiometric SrTiO-O<sub>2</sub> termination was considered because the other combinations were not electrically neutral.

In previous studies of the morphology of asymmetric tilt boundaries in SrTiO<sub>3</sub>,<sup>18</sup> the GB energy of the [001](100)/(430) asymmetric tilt GB was postulated to be about twice the value of the low-energy symmetric tilt GBs, suggesting that the asymmetric boundary was unstable. Our calculation, however, reveals that the nonstoichiometric asymmetric tilt GB with specific terminations can be as stable

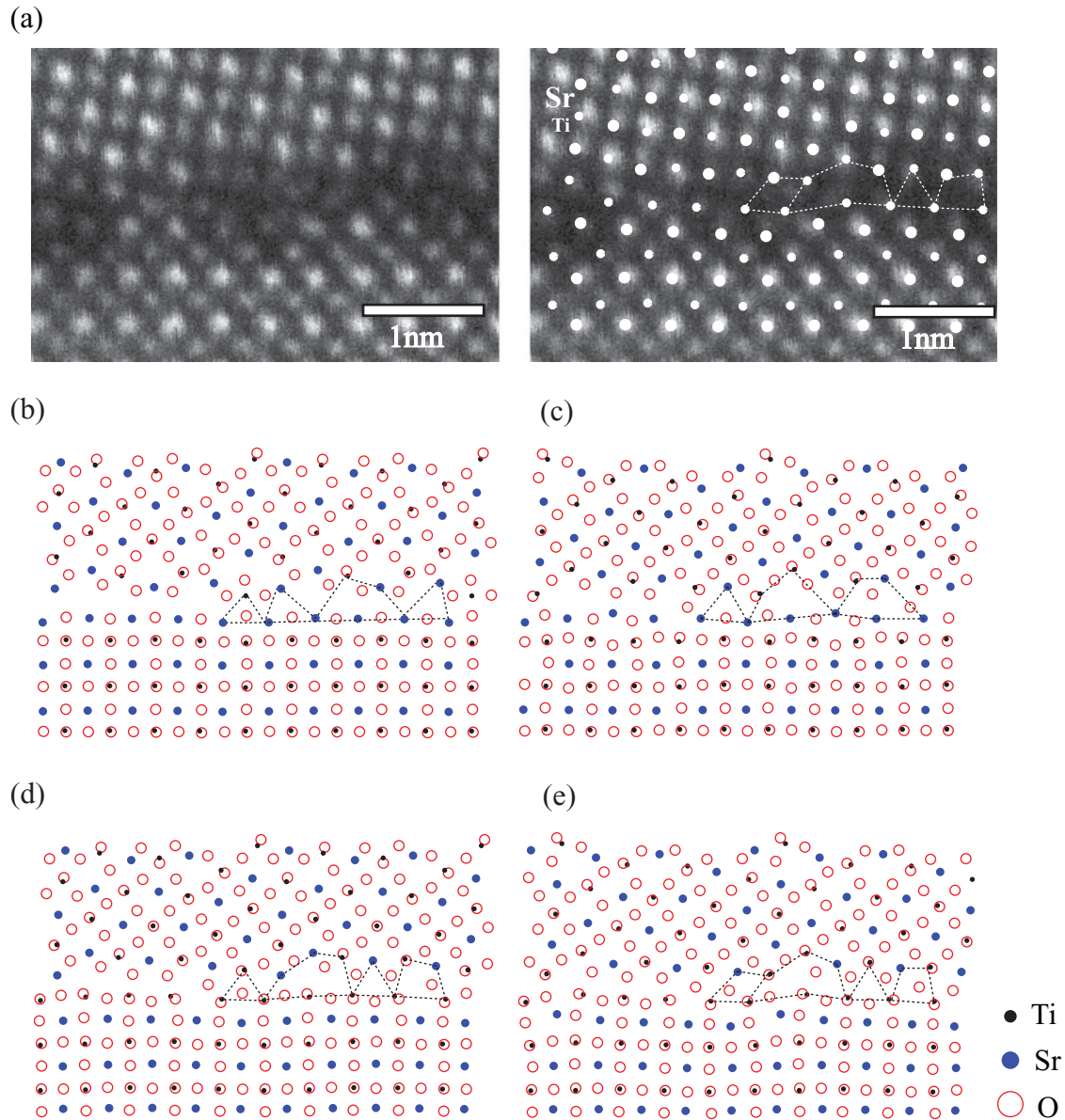


FIG. 4. (Color online) A HAADF-STEM image and the calculated structures of the asymmetric tilt  $[001](100)//(430)$   $\text{SrTiO}_3$  GB. (a) (left) HAADF-STEM image of  $\text{SrTiO}_3$  asymmetric GB. Because the intensity of the HAADF-STEM image is approximately proportional to the square of the atomic number, the brighter and darker columns correspond to Sr and Ti-O columns, respectively, whereas O columns are not seen (right). The atom positions are overlapped with the calculated Ti (small white dots) and Sr (large white dots) positions of the Ti-Ti terminated structure shown in (e). (b)–(e) The calculated most stable GB atomic structures for different terminations: (b) Sr-Sr, (c) Sr-Ti, (d) Ti-Sr, and (e) Ti-Ti.

as other symmetric tilt GBs. This result may explain why asymmetric boundaries are observed as frequently as symmetric boundaries in polycrystalline materials. The stability of our asymmetric tilt boundary has further been confirmed systematically with changing atmosphere. The results are described in the Sec. III C.

### B. Characterization of $[001](100)//(430)$ $\text{SrTiO}_3$ GB

To identify the atomic structure of the  $[001](100)//(430)$   $\text{SrTiO}_3$  GB experimentally, three different samples were observed by HAADF-STEM. Figure 4(a) shows a typical

HAADF-STEM image of the boundary. In this image, the brighter and darker spots in Fig. 4(a) correspond to Sr and Ti-O columns, respectively. It was found that the GB core consists of four structure units: a rhombus, a six-member polygon, a triangle, and a trapezium. The observed HAADF-STEM image was compared with the calculated stable structures of the four terminations shown in Figs. 4(b)–4(d). The Ti-Ti termination, which gives the lowest GB energy under the  $\text{TiO}_2$ -rich condition, was found to fit the observed structure best. According to previous studies,<sup>4,5,7,30</sup>  $\text{SrTiO}_3$  is in Ti-excess nonstoichiometry at high temperatures in air because the formation of Sr vacancies arises more readily than the

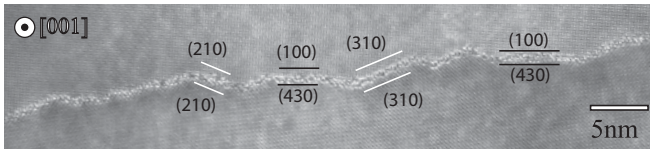


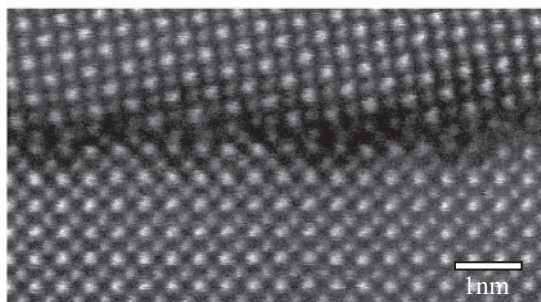
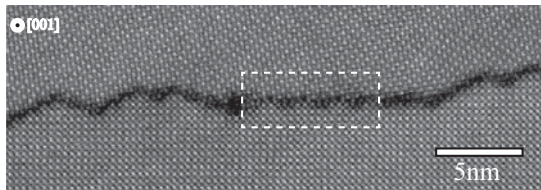
FIG. 5. HRTEM image of the joined [001](100)//(430) bicrystal before annealing.

formation of Ti vacancies. This result also supports our calculation and observation.

### C. The stability of asymmetric boundary at different oxygen partial pressures

It is commonly observed that an asymmetric GB consists of a few different inclination planes. After joining the [001](100)//(430) bicrystal, three major GB planes are observed, as shown in Fig. 5. An examination of their atomic structures and inclination angles revealed that the boundary consists

(a) in Air



(b) in H<sub>2</sub>

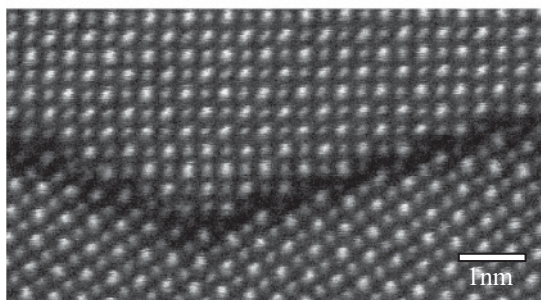
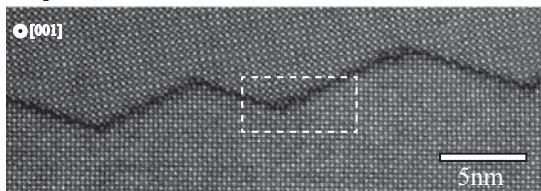


FIG. 6. HAADF-STEM images of the [001](100)//(430) bicrystal after annealing at 1350 °C for 120 hr (a) in air and (b) in H<sub>2</sub>.

of two symmetric tilt boundaries, [001] (210)  $\Sigma$ 5 and [001] (310)  $\Sigma$ 5, and one asymmetric boundary, the [001] (100)//(430) tilt boundary. In this study, it was found that the GB energy of the [001] (100)//(430) asymmetric tilt GB depends on the chemical potential of each element, whereas the GB energies of two symmetric tilt GBs are invariant with the oxygen partial pressure because they are stoichiometric.

The effect of the variation of the chemical potential of the elements on the GB structure was observed after annealing bicrystal specimens at 1350 °C for five days in different atmospheres of air and H<sub>2</sub>. Figures 6(a) and 6(b) show HAADF-STEM images of the specimens annealed in air and H<sub>2</sub>, respectively. To compare the GB structures in two different atmospheres quantitatively, the total lengths of three distinct GB planes were measured for more than 0.1 nm length of the GB for each specimen. An asymmetric tilt GB was not present in the H<sub>2</sub>-annealed specimen, whereas 15% of the GB length was the [001](100)//(430) asymmetric boundary in the air-annealed specimen. A DFT calculation showed that the energy of the [001](100)//(430) asymmetric boundary was 2.02 J/m<sup>2</sup> in a reducing atmosphere, in which the chemical potentials of Sr and Ti in SrTiO<sub>3</sub> are identical to those of metals. This value in air was 1.07 J/m<sup>2</sup>. This result indicates that in a reducing atmosphere, the [001](100)//(430) asymmetric boundary is energetically unstable and only two symmetric tilt GBs are stable. This result is in agreement with the experimental observation [Fig. 6(b)].

## IV. SUMMARY

In summary, an asymmetric tilt [001](100)//(430) SrTiO<sub>3</sub> GB was successfully modeled by the first-principles PAW method and experimentally confirmed by HAADF-STEM observations. The calculated energy of the asymmetric tilt GB was similar to those of symmetric tilt GBs under the Ti-excess or Sr-deficient condition. The present result can explain why the [001](100)//(430) SrTiO<sub>3</sub> GB is frequently observed in experiments and why this GB exists in a Ti-excess condition.<sup>5,18,21,31,32</sup> This study also demonstrates the method required to investigate the atomic structure and GB energy of asymmetric tilt GBs and provides an example to assist with a comprehensive understanding of asymmetric boundaries.

## ACKNOWLEDGMENTS

This work was supported in part by the Grant-in-Aid for Scientific Research on Priority Areas “Nano Materials Science for Atomic-Scale Modification 474”, A(70192474), Young Scientists (A) 22686059 and 23656395 from the Ministry of Education, Culture, Sports, and Technology (MEXT) of Japan. It was also partially supported by the special fund of Institute of Industrial Science, the University of Tokyo (5504850103) and by “MACAN (Grant No. 233484)” project funded by European Framework Programme 7 (FP7). Some calculations were performed by supercomputing system in Institute of Solid State Physics (ISSP), University of Tokyo (H23-Ba-0028, H23-Ba-0001).

\*teru@iis.u-tokyo.ac.jp

†ikuhara@sigma.t.u-tokyo.ac.jp

- <sup>1</sup>A. P. Sutton and R. W. Balluffi, *Interfaces in Crystalline Materials AP* (Oxford University Press, New York, 1995).
- <sup>2</sup>A. P. Sutton and V. Vitek, *Philos. Trans. R. Soc. London A* **309**, 1 (1983).
- <sup>3</sup>A. P. Sutton and V. Vitek, *Philos. Trans. R. Soc. London A* **309**, 37 (1983).
- <sup>4</sup>M. Imaeda, T. Mizoguchi, Y. Sato, H. S. Lee, S. D. Findlay, N. Shibata, T. Yamamoto, and Y. Ikuhara, *Phys. Rev. B* **78**, 245320 (2008).
- <sup>5</sup>H. S. Lee, T. Mizoguchi, J. Mitsui, T. Yamamoto, S. J. L. Kang, and Y. Ikuhara, *Phys. Rev. B* **83**, 104110 (2011).
- <sup>6</sup>M. M. McGibbon, N. D. Browning, M. F. Chisholm, A. J. McGibbon, S. J. Pennycook, V. Ravikumar, and V. P. Dravid, *Science* **266**, 102 (1994).
- <sup>7</sup>M. Kim, G. Duscher, N. D. Browning, K. Sohlberg, S. T. Pantelides, and S. J. Pennycook, *Phys. Rev. Lett.* **86**, 4056 (2001).
- <sup>8</sup>N. A. Benedek, Alvin L.-S. Chua, C. Elsasser, A. P. Sutton, and M. W. Finnis, *Phys. Rev. B* **78**, 064110 (2008).
- <sup>9</sup>A. L. S. Chua, N. A. Benedek, L. Chen, M. W. Finnis, and A. P. Sutton, *Nature Mater.* **9**, 418 (2010).
- <sup>10</sup>V. Ravikumar, V. P. Dravid, and D. Wolf, *Interface Sci.* **8**, 157 (2000).
- <sup>11</sup>V. P. Dravid and V. Ravikumar, *Interface Sci.* **8**, 177 (2000).
- <sup>12</sup>J. P. Buban, K. Matsunaga, J. Chen, N. Shibata, W. Y. Ching, T. Yamamoto, and Y. Ikuhara, *Science* **311**, 212 (2006).
- <sup>13</sup>F. Oba, H. Ohta, Y. Sato, H. Hosono, T. Yamamoto, and Y. Ikuhara, *Phys. Rev. B* **70**, 125415 (2004).
- <sup>14</sup>Y. Mishin, M. Asta, and J. Li, *Acta Mater.* **58**, 1117 (2010).
- <sup>15</sup>H. S. Lee, T. Mizoguchi, T. Yamamoto, S. J. L. Kang, and Y. Ikuhara, *Acta Mater.* **55**, 6535 (2007).
- <sup>16</sup>N. D. Browning, M. F. Chisholm, S. J. Pennycook, D. P. Norton, and D. H. Lowndes, *Physica C* **212**, 185 (1993).
- <sup>17</sup>T. Yamamoto, Y. Ikuhara, and T. Sakuma, *J. Mater. Sci. Lett.* **20**, 1827 (2001).
- <sup>18</sup>S. B. Lee and Y. M. Kim, *Acta Mater.* **57**, 5264 (2009).
- <sup>19</sup>T. Gemming, S. Nufer, W. Kurtz, and M. Ruhle, *J. Am. Ceram. Soc.* **86**, 581 (2003).
- <sup>20</sup>M. M. McGibbon, N. D. Browning, A. J. McGibbon, and S. J. Pennycook, *Philos. Mag. A* **73**, 625 (1996).
- <sup>21</sup>S. B. Lee, W. Sigle, W. Kurtz, and M. Ruhle, *Acta Mater.* **51**, 975 (2003).
- <sup>22</sup>S. B. Lee, W. Sigle, and M. Ruhle, *Acta Mater.* **51**, 4583 (2003).
- <sup>23</sup>H. Ichinose and Y. Ishida, *J. Phys.* **46**, 39 (1985).
- <sup>24</sup>A. Bourret, J. L. Rouviere, and J. M. Penisson, *Acta Crystallogr. Sect. A* **44**, 838 (1988).
- <sup>25</sup>K. L. Merkle, *Microsc. Microanal.* **3**, 339 (1997).
- <sup>26</sup>M. A. Tschopp and D. L. McDowell, *Philos. Mag.* **87**, 3147 (2007).
- <sup>27</sup>M. A. Tschopp and D. L. McDowell, *Philos. Mag.* **87**, 3871 (2007).
- <sup>28</sup>G. Kresse, Ph.D. thesis, Technische Universität, 1993.
- <sup>29</sup>G. Kresse and J. Furthmüller, *Comput. Mater. Sci.* **6**, 15 (1996).
- <sup>30</sup>T. Tanaka, K. Matsunaga, Y. Ikuhara, and T. Yamamoto, *Phys. Rev. B* **68**, 205213 (2003).
- <sup>31</sup>T. Yamamoto, Y. Sato, T. Tanaka, K. Hayashi, Y. Ikuhara, and T. Sakuma, *J. Mater. Sci.* **40**, 881 (2005).
- <sup>32</sup>T. Yamamoto and Y. Ikuhara, *J. Electron Microsc.* **50**, 485 (2001).